Inorganica Chimica Acta 376 (2011) 195–206

Contents lists available at ScienceDirect

Inorganica Chimica Acta

journal homepage: www.elsevier.com/locate/ica

Coordination polymers and monomers based on new aminocarboxylate ligands: A cadmium(II) polymer containing dimeric aqua-bridged cadmium complex governed by polymeric chain

Rampal Pandey [a], Mahendra Yadav [a], Prashant Kumar [a], Pei-Zhou Li [b], Sanjay Kumar Singh [b], Qiang Xu [b], Daya Shankar Pandey [a,*]

[a] Department of Chemistry, Faculty of Science, Banaras Hindu University, Varanasi 221005, U.P., India
[b] National Institute of Advanced Industrial Science and Technology (AIST), 1-8-31 Midorigaoka, Ikeda, Osaka 563-8577, Japan

ARTICLE INFO

Article history:
Received 12 February 2011
Received in revised form 24 May 2011
Accepted 8 June 2011
Available online 16 June 2011

Keywords:
Aminocarboxylates
Coordination polymers
Supramolecular assemblies
Fluorescence

ABSTRACT

The synthesis and characterization of novel coordination polymers $[Co(HCCB)(H_2O)_2]_n$ (**1**), $[Zn(HCCB)(H_2O)_2]_n$ (**2**), $\{[Cd(HCCB)_2]\cdot 0.5[Cd(\mu\text{-}H_2O)(H_2O)_4]_2\}_n$ (**3**) and $[Cu(HCCB)(H_2O)_2]_n$ (**4**) based on 3-(carboxymethylamino)-4-chlorobenzoic acid (H_3CCB) and mononuclear complexes $[Cu(HBCCB)(H_2O)]\cdot H_2O$ (**5**), $[Co(HBCCB)(H_2O)]\cdot H_2O$ (**6**), $[Zn(HBCCB)(H_2O)]$ (**7**) and $[Cd(HBCCB)(H_2O)]$ (**8**) containing 3-bis(carboxymethylamino)-4-chlorobenzoic acid (H_3BCCB) have been described. The compounds under investigation have been characterized by elemental analyses, spectral studies and structures of **1**–**3** and **5** determined crystallographically. Structural data of **1** and **2** revealed that the deprotonated $HCCB^{2-}$ bridges metal centers leading to a double stranded 1D chain. On the other hand, the $HCCB^{2-}$ coordinated thorough carboxylate oxygen and amino nitrogen in **3** to afford a 1D chain whose charge neutrality is maintained by inclusion of aqua-bridged dimer $[\{Cd(\mu\text{-}H_2O)(H_2O)_4\}_2]^{4+}$. Strong Cu···Cl interaction (2.754 Å) in **5** imposes a coordination geometry that is half-way between the square planar and square pyramidal. The H_3CCB, H_3BCCB and **1**–**3** and **5** are fluorescent at rt. Thermal studies (TG and DSC) on **1**–**3** suggested higher stability of **2** relative to **1** and **3** [ΔH_f (kcal/mol), ΔS_f = 152.17, 0.60, **1**; 195.56: 0.86, **2**; 69.33:0.36, **3**].

1. Introduction

The chemistry of coordination polymers have attracted a great deal of current attention owing to their intriguing molecular architectures, topologies and potential applications in various areas [1–8]. In this context, most of the work have been devoted toward rational design of metal–organic frameworks (MOFs) with specific structures and topologies displaying significant role in the development of functional materials with desirable properties [9–11]. During past few decades numerous coordination polymers have been successfully designed and synthesized through judicious choice of the organic ligands and metal ions [12–16]. It has been demonstrated that resultant structures are often affected by the geometry of metal ions, nature of the organic ligands, metal to ligand ratio, solvent employed, counter anions and the pH of reaction medium, etc. [17–20]. Among these, the choice of organic ligand plays a crucial role in their synthesis. In this regard, multidentate O-donor ligands especially organic aromatic polycarboxylates viz., 1,2-benzene-dicarboxylate, 1,3,5-benzenetricarboxylate, 1,2,4,5-benzenetetracarboxylate, etc., have drawn special attention [21,22]. In the construction of coordination polymers polycarboxylates are preferably employed as bridging ligand owing to their versatile coordination mode and high structural stability. Deprotonated carboxylates generally serve dual purpose, while acting as an anionic ligand to occupy the coordination sites, these also compensate overall charge [12,13,23,24].

The design and synthesis of novel coordination ligands is challenging and efforts are being made to tune the nature of interaction between reactants and metal ions to obtain desired structures [23–25]. To explore the possibility of formation of new coordination polymers, aminocarboxylate ligands 3-(carboxymethylamino)-4-chlorobenzoic acid (H_3CCB) and 3-(bis-carboxymethylamino)-4-chlorobenzoic acid (H_3BCCB) have been synthesized and used in the creation of coordination polymers and mononuclear complexes based on Co(II), Zn(II), Cd(II) and Cu(II). It is well documented that divalent zinc and cadmium ions frequently enhance structural diversity due to the lack of crystal field stabilization, which allows specific coordination environments responding to geometric and steric requirement of the carboxylate ligands [26]. Further, most often aqua ligand exhibits terminal coordination mode however, complexes containing aqua bridges are also known [27,28]. Although, a

---

* Corresponding author. Tel.: +91 542 7602480.
E-mail address: dspbhu@bhu.ac.in (D.S. Pandey).

0020-1693/$ - see front matter © 2011 Elsevier B.V. All rights reserved.
doi:10.1016/j.ica.2011.06.018

number of reports dealing with the coordination polymers based on Cd(II) have appeared in literature, the polymers containing co-crystallized aqua-bridged cadmium dimer governed by eight coordinated cadmium polymeric chain has not been described [29–33]. Through this work we present the synthesis and characterization of novel coordination polymers **1**–**4** based on H_3CCB, mononuclear complexes **5**–**8** containing H_3BCCB and crystal structures of **1**–**3** and **5**.

2. Experimental

2.1. Materials and general methods

The reagents were procured from commercial sources and used as received. Solvents were dried and distilled following the standard literature procedures [35]. IR and solid state electronic absorption spectra were recorded on a Perkin–Elmer-577 and Shimadzu UV-1701 spectrometers, respectively. ^1H NMR spectra in $CDCl_3$ was acquired on a JEOL AL 300 FT-NMR machine at an operating frequency of 300 MHz (^1H). Chemical shifts (δ) are given in parts per million (ppm) relative to tetramethylsilane (TMS, δ 0.00 ppm) and splitting patterns designated as s (singlet), d (doublet). Elemental analyses for C, H and N were performed on an Exter CE-440 CHN analyser. Thermogravimetric (TG) and differential scanning calorimetric (DSC) measurements were made on a Shimadzu DTG-60 simultaneous DTA-TG thermal analyzer at a heating rate of 1 °C/min^{-1} under nitrogen flow (generally 60 mL/min) and a Mettler Toledo DSC-25 with a flow rate of 30 mL/min, respectively. Crystalline samples were heated from ~25 to 600 °C at a rate of 10 °C/min.

2.2. Preparation of 3-(carboxymethyl-amino)-4-chlorobenzoic acid (H_3CCB)

An aqueous solution (10 mL) of 3-amino-4-chlorobenzoic acid (1.720 g, 10 mmol) was added dropwise to a solution of chloroacetic acid (1.880 g, 20.0 mmol) and KOH (1.120 g, 20.0 mmol) in water (15 mL) over half an hour and heated under reflux for 12 h. After cooling to room temperature it gave a white precipitate which was filtered, washed with water (20 mL) and air dried. Yield: 1.605 g, 69.8%. *Anal.* Calc. for $C_9H_8NO_4Cl$: C, 47.08; H, 3.51; N, 6.10. Found: C, 46.91; H, 3.49; N, 6.00%. ^1H NMR (D_2O, δ ppm): 7.40 (d, 1H), 7.21 (d, 1H), 6.99 (s, 1H), 3.66 (s, 1H), 3.67 (s, 2H). IR data (KBr pellet, cm^{-1}): 3404 s, 1689 s, 1597s, 1511 m, 1452 m, 1352 m, 1302 s, 1269 s, 1038 m, 758 s. UV–Vis (solid state, λ_{max} nm): 360, 303.

2.3. Preparation of 3-(bis-carboxymethyl-amino)-4-chlorobenzoic acid (H_3BCCB)

The filtrate obtained after separation of H_3CCB upon neutralization with 0.01 M HCl gave H_3BCCB as a white solid which was separated by filtration, washed with 3 × 20 mL of water and air dried. Yield: 41.2% (1.188 g). *Anal.* Calc. for $C_9H_8NO_4Cl$: C, 45.93, H, 3.50, N, 4.87. Found: C, 45.71; H, 3.38; N, 4.80%. ^1H NMR (D_2O, δ ppm): 7.41 (d, 1H), 7.30 (d, 1H), 7.09 (s, 1H), 3.67 (s, 4H). IR (KBr pellet, cm^{-1}): 3410 br, 1736 vs 1681 vs 1597s, 1437 s, 1291 s, 1230 m, 1154 m, 1037 m, 867 w, 764 s. UV–Vis (H_2O, λ_{max} nm): 242, 210.

2.4. Preparation of $[Co(HCCB)(H_2O)_2]_n$ **1**

A mixture of $Co(NO_3)_2{\cdot}6H_2O$ (0.291 g, 1.0 mmol), H_3CCB (0.230 g, 1.0 mmol) and KOH (0.112 g, 2.0 mmol) in H_2O (8 mL) were heated in a sealed tube at 120 °C for 24 h. Upon cooling to room temperature it afforded dark pink block shaped crystals suitable for X-ray diffraction analyses, which were collected by filtration, washed with water/ethanol (1:1) and dried in air. Yield: 0.194 g, 60.2%. *Anal.* Calc. for $C_9H_{10}NO_6ClCo$: C, 33.5; H 3.12; N, 4.34%. Found: C, 33.39; H, 3.02; N, 4.22%. IR (KBr pellet, cm^{-1}): 1610 s, 1551 s, 1382 s, 1340 m, 1245 w, 1035 m, 781 s. UV–Vis (solid state, λ_{max} nm): 295, 543.

2.5. Preparation of $[Zn(HCCB)(H_2O)]_n$ **2**

It was synthesized following the above procedure for **1** except that $Zn(NO_3)_2{\cdot}6H_2O$ (0.297 g, 1 mmol) was used in place of $Co(NO_3)_2{\cdot}6H_2O$. Diffraction quality dirty white block shaped crystals of **2** were obtained from the reaction mixture after cooling to room temperature. These were separated by filtration, washed with water/ethanol (1:1) and dried in air. Yield: 64.4% (0.419 g). *Anal.* Calc. for $C_{18}H_{14}N_2O_{12}Cl_2Zn_2$: C, 33.19; H, 2.18; N, 4.36. Found: C, 33.08; H, 2.12; N, 4.26%. IR (KBr pellet, cm^{-1}): 1615 s, 1558 s, 1377 s, 1342 m, 1245 w, 1036 m, 779 s. UV–Vis (solid state, λ_{max} nm): 270, 319.

2.6. Preparation of $\{[Cd(HCCB)_2]{\cdot}0.5[Cd(\mu\text{-}H_2O)(H_2O)_4]_2\}_n$ **3**

It was prepared following the above procedure for **1** using $Cd(NO_3)_2{\cdot}4H_2O$ (0.308 g, 1 mmol) in place of $Co(NO_3)_2{\cdot}6H_2O$. Colorless block shaped crystals of **3** were separated by filtration, washed with water/ethanol (1:1) and dried in air. Yield: 0.448 g, 59.0%. *Anal.* Calc. for $C_{18}H_{14}N_2O_{13}Cl_2Cd_2$: C, 28.49; H, 1.60; N, 3.72. Found: C, 28.38; H, 1.49; N, 3.64%. IR (KBr pellet, cm^{-1}): 1590 s, 1552 s, 1384 s, 1313 m, 1229 w, 1037 m, 792 s, 677 m. UV–Vis (solid state, λ_{max} nm): 270, 319.

2.7. Preparation of $[Cu(HCCB)(H_2O)]_n$ **4**

It was prepared following the above procedure for **1** except that $Cu(NO_3)_2{\cdot}3H_2O$ (0.232 g, 1 mmol) was used in place of $Co(NO_3)_2{\cdot}6H_2O$. It isolated as gray crystalline solid from the reaction mixture after cooling to room temperature and was separated by filtration, washed with water/ethanol (1:1) and dried in air. Yield: 74.1% (0.479 g). *Anal.* Calc. for $C_{18}H_{14}N_2O_{12}Cl_2Zn_2$: C, 33.35; H, 2.18; N, 4.32. Found: C, 33.18; H, 2.06; N, 4.24%. IR (KBr pellet, cm^{-1}): 3226 m, 1626 s, 1565 s, 1429, 1385 s, 1325 m, 1269 w, 1044 m, 763 s. UV–Vis (solid state, λ_{max} nm): 270, 319.

2.8. Preparation of $[Cu(HBCCB)(H_2O)]{\cdot}H_2O$ **5**

A mixture containing $Cu(NO_3)_2{\cdot}3H_2O$ (0.232 g, 1.0 mmol), H_3BCCB (0.288 g, 1.0 mmol), KOH (0.112 g, 2.0 mmol) in H_2O (8 mL) was heated at 120 °C in a sealed tube for 24 h. Dark blue block shaped crystals of **5** suitable for X-ray diffraction analysis were obtained after cooling the reaction mixture to room temperature. Yield: 0.243 g, 69%. *Anal.* Calc. for $C_{11}H_{12}ClCuNO_8$: C, 34.30; H, 3.14; N, 3.64. Found: C, 34.18; H, 3.02; N, 3.52%. IR (KBr pellet, cm^{-1}): 1721 s, 1610 vs 1385 vs 1250 m, 935 m, 763 m. UV–Vis (H_2O, λ_{max} nm): 263, 215.

2.9. Preparation of $[Co(HBCCB)(H_2O)]{\cdot}H_2O$ **6**

It was prepared following the above procedure for **4** using $Co(NO_3)_2{\cdot}6H_2O$ (0.291 g, 1.0 mmol) in place of $Cu(NO_3)_2{\cdot}3H_2O$. It isolated as pink crystalline solid which was separated by filtration, washed with water/ethanol (1:1) and dried in air. Yield: 0.213 g, 56.2%. *Anal.* Calc. for $C_{11}H_{12}ClCoNO_8$: C, 34.71; H, 3.18; N, 3.68. Found: C, 34.45; H, 3.10; N, 3.55%. IR (KBr pellet, cm^{-1}): 1714 s, 1610 vs 1381 vs 1256 m, 1182, 931 m, 753 m.

2.10. Preparation of [Zn(HBCCB)H_2O] **7**

It was prepared following the above procedure for **4** using $Zn(NO_3)_2 \cdot 6H_2O$ (0.297 g, 1.0 mmol) in place of $Cu(NO_3)_2 \cdot 3H_2O$. After cooling the reaction mixture to room temperature it separated as the white solid which was collected by filtration, washed with water/ethanol (1:1) and air dried. Yield: 0.193 g, 52.5%. *Anal.* Calc. for $C_{11}H_{10}ClZnNO_7$: C, 35.80; H, 2.73; N, 3.80. Found: C, 35.55; H, 2.61; N, 3.68%. IR (KBr pellet, cm^{-1}): 1689 s, 1606 vs 1386 vs 1263 m, 1206, 935 m, 776 m.

2.11. Preparation of [Cd(HBCCB)H_2O] **8**

It was prepared following the above procedure for **4** using $Cd(NO_3)_2 \cdot 4H_2O$ (0.308 g, 1.0 mmol) in place of $Cu(NO_3)_2 \cdot 3H_2O$. The complex **8** separated as white powder upon cooling the reaction mixture to room temperature and was collected by filtration, washed with water/ethanol (1:1) and dried in air. Yield: 0.209 g, 50.3%. *Anal.* Calc. for $C_{11}H_{10}ClCdNO_7$: C, 31.75; H, 2.42; N, 3.37. Found: C, 31.57; H, 2.37; N, 3.28%. IR (KBr pellet, cm^{-1}): 1706 s, 1598 vs 1386 vs 1267 m, 1203, 933 m, 766 m.

2.12. X-ray structure determinations

Single crystal X-ray data for **1**, **2**, **3** and **5** were collected on a Rigaku R-AXIS RAPID II diffractometer at room temperature using graphite-monochromated Mo Kα radiation (λ = 0.71073 Å). The crystallographic and refinement data for **1**, **2**, **3** and **5** are summarized in Table 1. Structures were solved by direct methods (SHELXS 97) and refined by full-matrix least squares on F^2 (SHELX 97) [36,37]. Non-hydrogen atoms were refined with anisotropic thermal parameters. All the hydrogen atoms were geometrically fixed and refined using a riding model. Computer program PLATON was used for analyzing the interaction and stacking distances [38,39]. Powder X-ray diffraction data for **4** and **6**–**8** (PXRD) were obtained on a Rigaku Rotoflux RTC-300 X-ray diffractometer employing Cu Kα (λ = 1.5406 Å) radiation with a Ni filter.

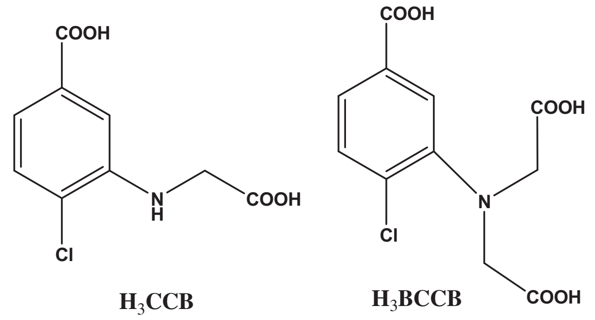

Fig. 1. Structures of the ligands.

3. Results and discussion

3.1. Syntheses and characterization

The ligands H_3CCB and H_3BCCB were prepared by reaction of 3-amino-4-chlorobenzoic acid with chloroacetic acid under alkaline conditions. Presence of both the aminocarboxylate (–N–CH_2–COOH) and carboxylate group enables it to form covalent/coordination bonds with the metal ions either through nitrogen and carboxyl oxygen of the former or oxygen of the latter after deprotonation (Fig. 1). Further, carboxyl oxygen and nitrogen may easily get involved in intra- and intermolecular hydrogen bonding interactions.

The complexes **1**–**4** were synthesized using H_3CCB and metal(II) nitrates under carefully controlled conditions (metal:ligand; 1:1, 120 °C). Treatment of the hydrated metal nitrates $Co(NO_3)_2 \cdot 6H_2O$, $Zn(NO_3)_2 \cdot 6H_2O$ and $Cu(NO_3)_2 \cdot 3H_2O$ with H_3CCB under alkaline conditions afforded double-stranded 1D coordination polymers $[Co(HCCB)(H_2O)]_n$ (**1**), $[Zn(HCCB)(H_2O)]_n$ (**2**) and $[Cu(HCCB)(H_2O)]_n$ (**4**). On the other hand, $Cd(NO_3)_2 \cdot 4H_2O$ reacted with H_3CCB under analogous conditions to give entirely different complex $\{[Cd(HCCB)]_2 \cdot 0.5[Cd(\mu\text{-}H_2O)\text{-}(H_2O)_4]_2\}_n$ (**3**). Although **1**–**4** have been synthesized essentially under identical conditions, these exhibit structural diversity, wherein both the aminocarboxylate and

Table 1
Crystal and structure refinement data for **1**–**3** and **5**.

Compound	1	2	3	5
CCDC numbers	743 407	747 607	747 608	787 720
Empirical formula	$C_9H_{10}ClCoNO_6$	$C_{18}H_{14}Cl_2N_2O_{12}Zn_2$	$C_{18}H_{12}Cd_2Cl_2N_2O_{13}$	$C_{24}H_{24}Cl_2Cu_2N_2O_{16}$
Formula weight	322.56	651.95	760.00	794.43
Crystal system	triclinic	triclinic	triclinic	triclinic
Space group	$P\bar{1}$	$P\bar{1}$	$P\bar{1}$	$P\bar{1}$
a (Å)	6.870(1)	6.860(1)	8.053(2)	7.493(2)
b (Å)	7.573(2)	10.699(2)	8.223(2)	7.791(2)
c (Å)	10.723(2)	15.073(3)	18.733(4)	13.097(3)
α (°)	89.21(3)	88.94(3)	89.74(3)	84.71(3)
β (°)	89.41(3)	82.62(3)	78.98(3)	75.49(3)
γ (°)	77.86(3)	89.72(3)	80.54(3)	69.52(3)
V (Å^3)	545.2(2)	1096.9(4)	1200.5(4)	693.4(3)
Z	2	2	2	1
T (K)	293	293	293	293
μ (mm^{-1})	1.838	2.502	2.065	1.812
D_{calc} (g/cm^3)	1.964	1.974	2.103	1.902
Reflections collected	5337	10 626	11 405	2569
Independent reflections	2465	4950	5368	3147
R_{int}	0.0386	0.0754	0.0937	0.0407
wR_2 (all data)	0.0920	0.2039	0.2417	0.1069
Goodness-of-fit (GOF) on F^2	1.224	1.064	1.051	1.078

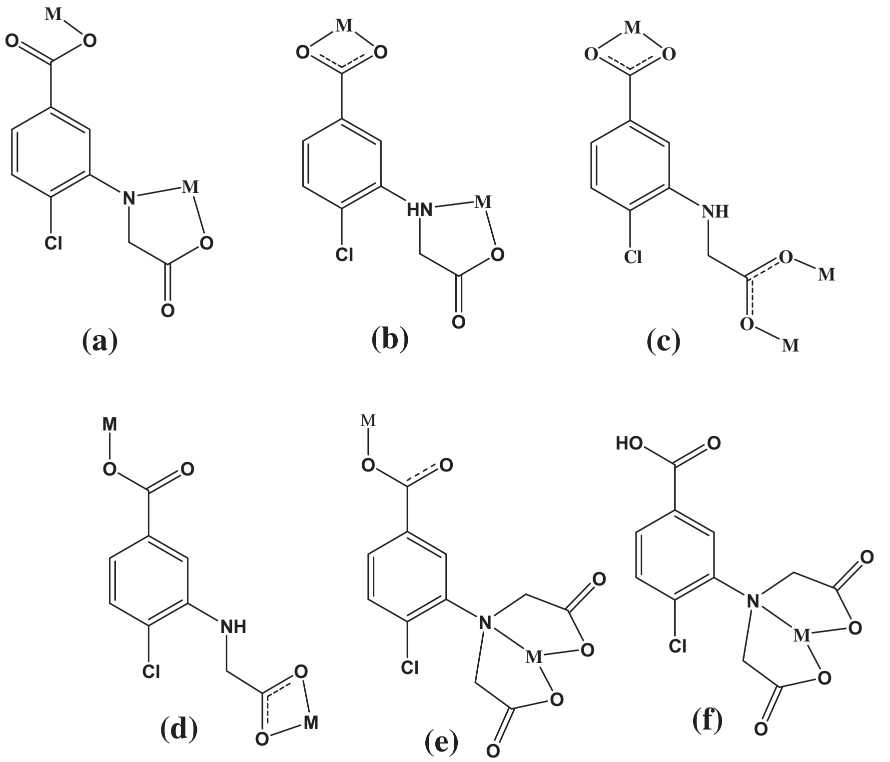

Scheme 1. (a) and (b) coordination mode of H_3CCB in complexes **1**–**4**. (c–e) Other possible coordination modes of H_3CCB and H_3BCCB (f) coordination mode of H_3BCCB in complexes **5**–**8**.

carboxylate groups of H_3CCB are involved in bonding with the metal centers (Scheme 1).

Under analogous conditions $Cu(NO_3)_2{\cdot}3H_2O$, $Co(NO_3)_2{\cdot}6H_2O$, $Zn(NO_3)_2{\cdot}6H_2O$ and $Cd(NO_3)_2{\cdot}6H_2O$ reacted with H_3BCCB (metal:ligand; 1:1, 120 °C) to afford mononuclear complexes $[Cu(HBCCB)(H_2O)]{\cdot}H_2O$ (**5**) $[Co(HBCCB)(H_2O)]{\cdot}H_2O$ (**6**), $[Zn(HBCCB)H_2O]$ (**7**) and $[Cd(HBCCB)H_2O]$ (**8**) in moderate to good yields. In **5**–**8** the ligand H_3BCCB interacted with the metal center through aminocarboxylate group, while carboxylate group remains uncoordinated (Scheme 1e).

Characterization of the ligands and **1**–**8** have been achieved by elemental analyses, spectral (FT-IR, ^1H NMR, electronic absorption, emission) and thermal (TG and DSC) studies. The structures of coordination polymers **1**–**3** and representative mononuclear complex **5** have been determined by single crystal X-ray diffraction analyses. Information about the structures of **4** and **6**–**8** have also been obtained by comparing their powder X-ray patterns (PXRD) with the simulated patterns from single crystal X-ray data of **1** and **5**.

3.2. Crystal structures of $[Co(HCCB)(H_2O)_2]_n$ 1 and $[Zn(HCCB)(H_2O)]_n$ 2

Coordination polymers **1** and **2** crystallize in triclinic crystal system and $P\bar{1}$ space group. The asymmetric units of these consists of two metal ions (Co, **1**; and Zn, **2**), two deprotonated ligands ($HCCB^{2-}$) and four water molecules. Coordination geometry about the metal centers in both **1** and **2** is distorted octahedral wherein Co(II)/Zn(II) are coordinated by three oxygen donors from three different carboxylates, amino nitrogen and two water molecules (Figs. 2a and 3a). The ligand H_3CCB in its deprotonated form ($HCCB^{2-}$ coordinated to the respective metal center in two different modes: (i) the aminocarboxylate interacted with two different metal centers in μ–η2–O(1), η1–N(1) mode, (ii) carboxylate group bonded through carboxyl oxygen in monodentate η1–O(4) fashion. The ligand moieties in asymmetric unit assume "*anti*, *anti*" orientation. Each of the Co(II)/Zn(II) centers are connected with two bridging ligands to form a 14-membered macrocycle thus the structure of **1** and **2** can be best described as a double stranded looped-chain 1D coordination polymer (Figs. 2a and 3a). Two types of metal–metal distances occur in double stranded chain of **1** and **2**; (i) separated by bridging oxygen of the carboxylate groups (3.241 Å in **1**; 3.294 Å in **2**) and (ii) separated by $HCCB^{2-}$ 8.561 Å in **1**; 8.479 Å in **2**) as shown in Scheme 2. The Co–O(carboxylate/aminocarboxylate) and Co–O(w) bond distances in **1** fall in the range of 2.057(3)–2.049(3) and 2.084(4)–2.121(4) Å. Similarly, Zn–O(carboxylate-/aminocarboxylate), Zn–O(w) bond distances in **2** are in the range of 2.031(4)–2.094(4), 1.984(4)–2.054(4) Å. The Co–N and Zn–N bond distances are 2.249(4) Å and 2.208(5)–2.255(4) Å, respectively. These are normal and comparable to the bond distances observed in other related systems [40–42]. The O(5)–Co(1)–O(6) and O(5)–Zn(1)–O(11)/O(8)–Zn(2)–O(7) angles in **1** and **2** are 86.60(18) and 95.61(16)–87.69(16)°. It suggested that the coordinated water molecules are *cis*-disposed about the Co(II)/Zn(II) throughout polymeric chain. Complexes, **1** and **2** differ in empirical formula due to dissimilar symmetry codes (Figs. 2a and 3a).

The N(1)–C(2)–C(1) and N(2)–C(11)–C(10) angles in **1** and **2** are 113.4(4)° and 112.4(4)°, which strongly suggested that the N,O donor sites of aminocarboxylate are almost planar with respect to each other. The Co(1)–$O(1)_{brid}$–Co(1) and Zn(1)–$O(1)_{brid}$–Zn(2) angles are 101.36(14)° and 103.53(2)°, respectively. An examination of the crystal structures of **1** and **2** revealed the presence of two types of cavities in their polymeric chain. Square shaped cavities of the dimension [2.656(4) × 3.241(6) Å^2, **1**; 2.615(4) × 3.294(4) Å^2, **2**], created between two nearest metal centers separated by V-shaped oxygen bridges of the ligand in polymeric chain. Dimension has been measured by considering M···M (Co···Co/Zn···Zn) × O(1)···O(1) distances. Ellipsoid cavities of the dimension [5.241 × 8.561 Å^2, **1**; 5.206 (3) × 8.479 (2) Å^2, **2**] are formed between two M···M (Co···Co/Zn···Zn) centers separated by

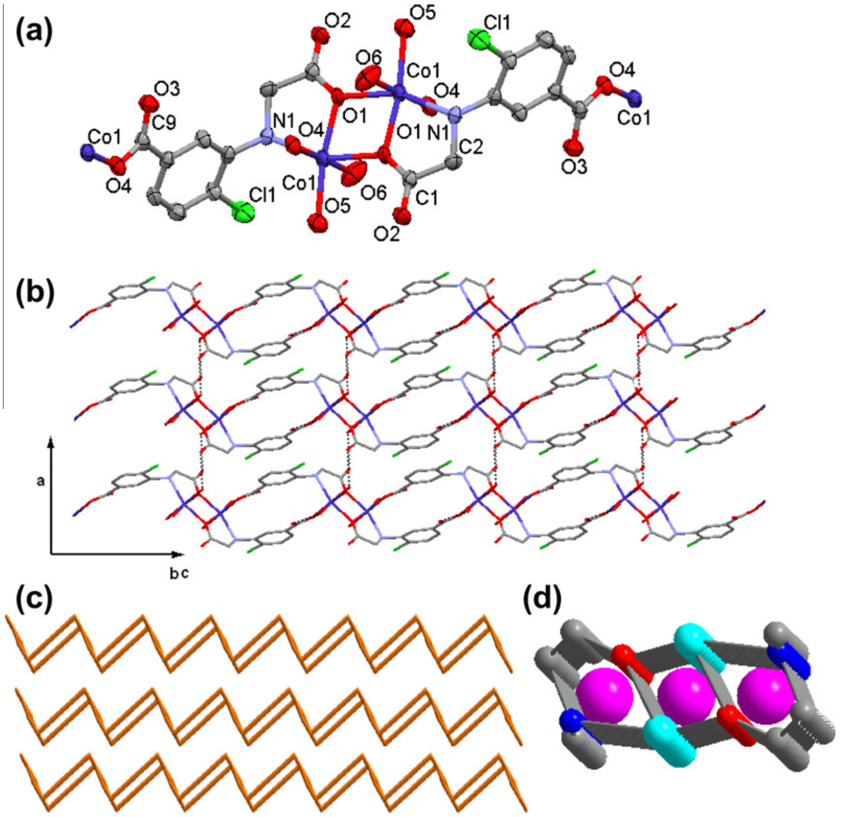

Fig. 2. (a) Crystal structure of **1** (hydrogen atoms omitted for clarity), Symmetry codes: i) *x*, *y*, *z*-1; ii) *x*, *y*, *z* + 1; iii) -*x*, -*y* + 1, -*z* + 1. (b) Overall 2D structure of **1** resulted by intermolecular hydrogen bonding interactions. (c) A topological representation for 2D zig-zag double stranded chains in **1** through π–π stacking interactions. (d) Cavities created in **1** viewed down along crystallographic-‘*b*’ axis.

$HCCB^{2-}$ in the double stranded chains (Scheme 2). Dimension has been calculated by distances between M···M (Co···Co/Zn···Zn) separated by ligands × centroid–centroid of the aromatic rings of the bridged ligands.

3.3. Supramolecular assemblies through weak bonding interactions

Double stranded chain lies parallel to each other through hydrogen bonding, C–H···π and π–π interactions leading to 2D layers in the *bc*-plane. Intermolecular O–H···O hydrogen bonding interactions in **1** and **2** leads to two dimensional (2D) repeated double stranded chains along the crystallographic *c*-axis (Figs. 2b and 3b, Table 3). The distance(s) between Co···Co/Zn···Zn centers separated by $HCCB^{2-}$ in the chains are 6.870/7.564 Å. The intra- and intermolecular hydrogen bonding distances are 2.570 and 3.048 Å, in **1** and 2.597 and 2.829 Å in **2**, respectively [1,2]. Zig-zag parallel chains with ellipsoidal cavities have been created from C–H···π and π–π interactions in **1** leading to a 2D network along crystallographic *c*-axis (Fig. 2c, S2 and S3, ESI). These interactions in **2** lead to three parallel chains with ellipsoidal cavities along crystallographic *c*-axis (Fig. 3c, S4). Intra- and intermolecular C–H···π distances (measured from hydrogen to centroid of the aromatic ring) are 3.311 and 3.473 Å, respectively in **1**. Although, **1** and **2** have got similar structural framework, intramolecular C–H···π interactions are lacking in **2**. Intra- and intermolecular π–π stacking distances are 3.135 and 3.299 Å in **1** and 3.168 and 3.394 Å in **2**, respectively. The centroid–centroid distances between aromatic rings of $HCCB^{2-}$ bridging two metal centers in **1** and **2** are 5.241 and 5.206 Å while, intra- and inter-chain aromatic ring (centroid–centroid) distances are 4.415 and 4.586 Å. Shorter inter-chain distances in comparison to intra chain separations certainly contribute towards overall stability of the 2D chains in **1** and **2**.

The nearest Co···Co separations in **1** are 3.241, whereas Zn···Zn distances in **2** are 3.294 Å (Scheme 2). Slightly longer distances in **2** may be due to smaller ionic radii of Zn(II) in comparison to Co(II). Distances between μO(1)···μO(9) in **1** and **2** are 2.656 and 2.615 Å, respectively. All the oxygen atoms of both **1** and **2** are involved either in intra- or intermolecular hydrogen bonding interactions (Table 3). Notably, these compounds contain both the Lewis basic (the non-coordinated oxygen atoms) and acidic centers (the coordinated Co(II)/Zn(II) ions with potentially good leaving coordinated water molecules) in the same unit, may find potential application as a bifunctional catalyst [43,44].

3.4. Crystal structures of $\{[Cd(HL1)_2]\cdot 0.5[Cd(\mu\text{-}H_2O)(H_2O)4]2\}_n$ **3**

The crystallographic data of **3** suggested that it belongs to triclinic crystal system with $P\bar{1}$ space group. Its overall structure shows 1D polymeric chain containing Cd(II) and $HCCB^{2-}$ alongwith rhomboid dimeric cationic species $[\{Cd(\mu\text{-}H_2O)(H_2O)_4\}_2]^{4+}$ held between two polymeric chains. Cadmium in the polymeric chains are eight, while those in dimeric unit are six coordinated [32,33]. The local coordination environment about Cd(1) can be best described as a distorted tetragonal antiprism consisting of six oxygen from four different carboxylate groups of $HCCB^{2-}$, adopting k^2-COO^- and k^1-COO^- coordination mode and two nitrogen from different ligands (Fig. 4a). The polymeric part incorporating bridging $HCCB^{2-}$ creates a 14-membered macrocyclic ring alongwith rhomboid dimeric unit, can also be ascribed as a double stranded looped chain. The Cd–O distances (range 2.310(9)–2.630(11) Å) are similar to those in other eight coordinated Cd(II) complexes [45,46].

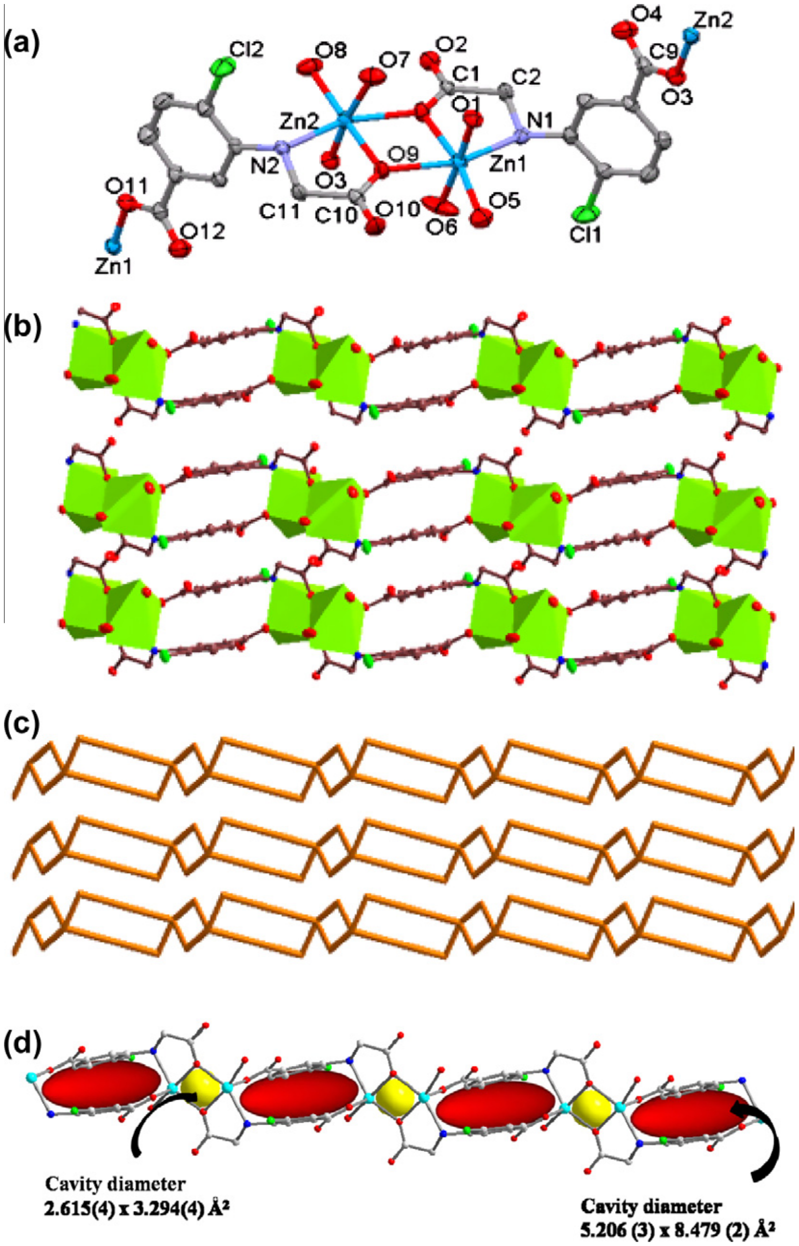

Fig. 3. (a) Crystal structure of **2** (hydrogen atoms omitted for clarity), Symmetry codes: i) *x*, *y*-1, *z*; ii) *x*, *y* + 1, *z*. (b) Overall 2D structure of **2** resulted by O-H···O hydrogen bonding interactions. (c) Topological representation for three parallel ribbons generated from $\pi\cdots\pi$ interactions. (d) Two types of cavities differing in dimensions along crystallographic-'*c*' axis.

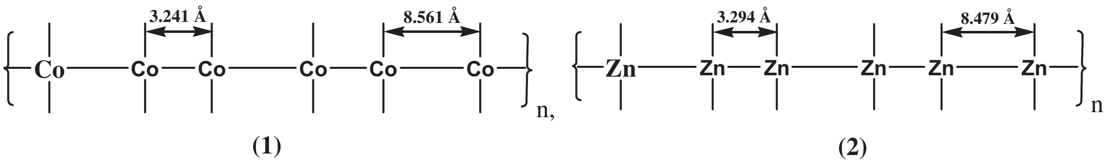

Scheme 2. Metal–metal distances in two types of cavities present in the polymeric double stranded chain of **1** and **2**.

The Cd(1)–N(1) and Cd(1)–N(2) distances are 2.651(11) and 2.572(12) Å, respectively which are comparable to those reported in the literature [47,48]. The distorted octahedral coordination geometry about Cd(2) is completed by four terminal and two bridging aqua ligands (Fig. 4a and S6). This type of coordination environment around Cd(II) in the same complex have not been observed so far to the best of our knowledge in cadmium(II) polycarboxylate MOFs [32,33,49–51]. One can see that each ligand connects two metal centers through three oxygens of the carboxylate group coordinated in k^1-COO$^-$ and k^2-COO$^-$ modes and the nitrogen (Fig. 4a). Each Cd(1) in the polymeric chains are bonded to four HCCB^{2-} and forms a 1D chain, which in association with

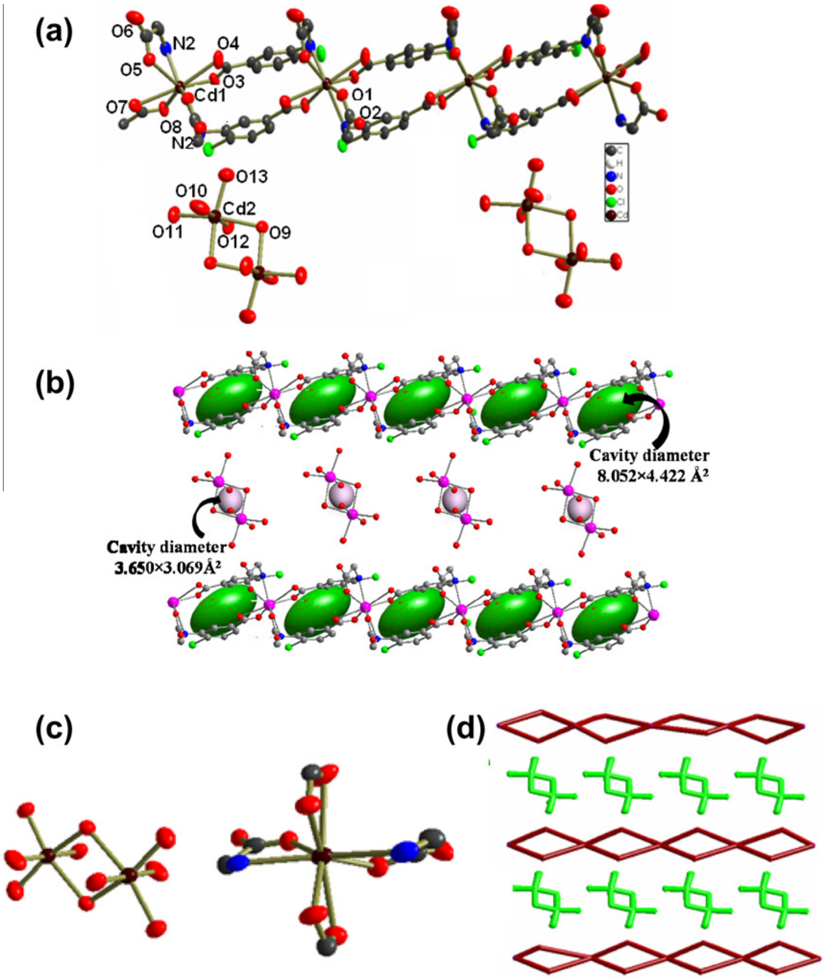

Fig. 4. (a) Crystal structure of **3** (hydrogen atoms omitted for clarity), Symmetry code: i) -*x* + 1, -*y*, -*z* + 1; ii) *x*-1, *y*, *z*; iii) *x* + 1, *y*, *z*.; (b) Ellipsoidal (polymeric part) and squire shape cavities (dimeric part) viewed down along crystallographic-'*c*' axis. (c) Arrangement of various atoms about Cd(1) and Cd(2). (d) Topological representation of dimeric cadmium complex sandwiched between infinite double stranded chains in **3**.

symmetrical aqua-bridged dimeric species leads to a 1D framework and weak intermolecular interactions generate 2D as well as 3D supramolecular network. According to the simplification principle, the ligand $HCCB^{2-}$ in **3** can be viewed as a connector and Cd(II) as four-connected nodes.

The carboxylate groups having similar coordination mode (k^1 or k^2) are *trans*-disposed. Aqua-bridged dimeric Cd(II) complex does not contain H_3CCB and completed its distorted octahedral geometry by aqua ligand in both the bridged and terminal mode. The Cd–$O_{terminal}$ bond distances lie in the range 2.211(10)–2.236(10) Å, while Cd–$O_{bridged}$ are 2.357(8) Å. Comparison of bond distances revealed that the Cd(2)–$O(9)_{bridged}$ are longer than Cd(2)–$O_{terminal}$. Unlike **1** and **2**, the complex **3** contains only ellipsoidal cavities generated by neighboring Cd(II) bridged by $HCCB^{2-}$ in the polymeric double stranded looped chain. In this complex Cd(1) are separated from each other by 8.053 and Cd(2) by 3.650 Å.

The 1D double stranded 14-membered chain in **3** stacked along crystallographic *b*-axis leading to a 3D supramolecular architecture *via* strong O–H···O hydrogen bonding interactions involving μ-aqua and terminal water molecules (O9, O10, O11, O12 and O13) of the rhomboid dimers (Fig. 5a, S8, Table 3). Intermolecular C–H···π interactions (3.421(2) Å) in the polymeric chain generated a 2D layered network along crystallographic *a*-axis (Fig. 5d). Further, **3** lacks inter-chain contacts through π–π interactions, however, intramolecular π–π stacking interactions (3.29 Å) are present (Fig. S5). The absence of inter-chain contacts through π–π interactions may be attributed to the presence of dimeric units between two polymeric chains. Intra-layer distances between the centroids of aromatic ring of the ligand bridging two Cd(II) centers are 5.241 Å, whereas inter-chain centroid–centroid distances are 4.415 Å. This type of contact contributes towards stability of the chain.

As described above, **1** and **2** adopted analogous, while **3** an entirely different structure. The difference in overall structures may be related to ability of the cadmium (4*d* metal) to adopt higher coordination numbers. It is well established that Cd(II) in its complexes can adopt coordination number 6–9 [52,53]. An inspection of the structure of **3** revealed that each Cd(II) is linked to two $HCCB^{2-}$ through nitrogen and oxygen of the aminocarboxylate and other two through both the oxygen of carboxylate group after deprotonation. The coordination of $HCCB^{2-}$ accumulates four negative charge on each cadmium center in the polymeric chain. Cadmium generally do not show oxidation states higher than two, while from crystal structure it is obvious that each Cd(II) in the polymeric chain bears four net negative charges. To balance the charge in polymeric chain, aqua-bridged dimeric complex bearing two net positive charges on each Cd(II) co-crystallizes with the polymeric chain (observed dimeric/polymeric ratio; 0.5:1.0). Among these three coordination polymers **3** is least stable. It may be attributed to the easier collapse of aqua-bridged dimeric

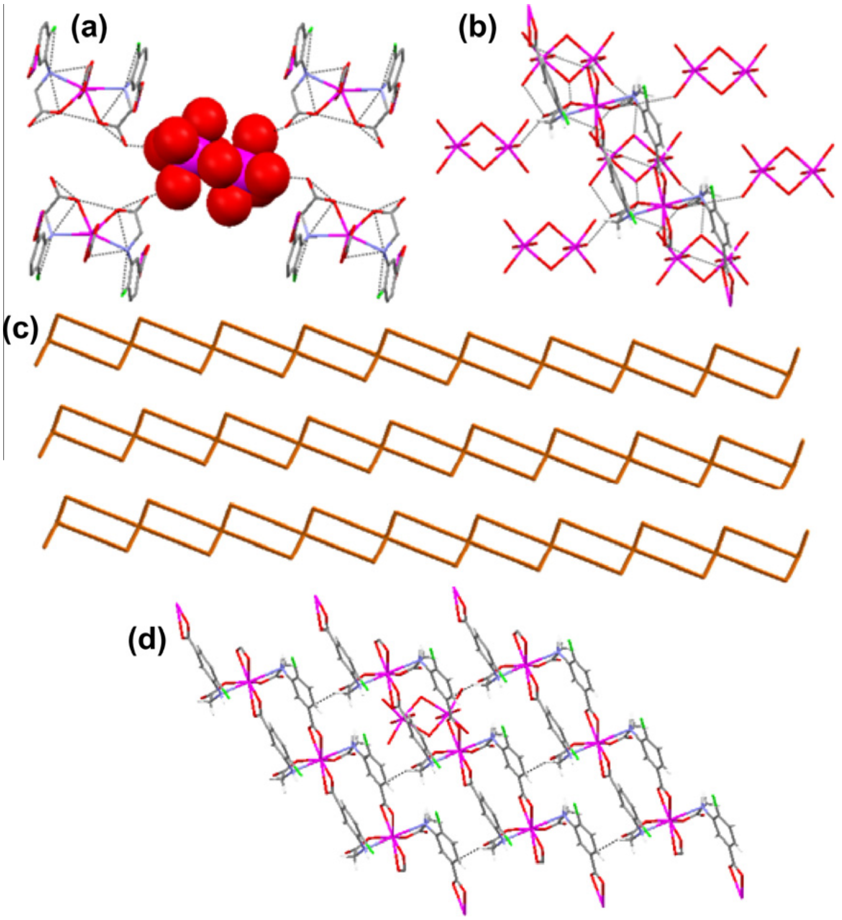

Fig. 5. (a) Environment of polymeric chains about cadmium centers in dimeric part. (b) Cadmium dimers about polymeric chain. (c) Topological view of the polymeric chains with ellipsoidal cavities. (d) A 2D layered network constructed by CH···π contacts.

moiety as well as steric crowding around the Cd(II) in polymeric chain.

3.5. Structure of [Cu(HBCCB)(H_2O)]·H_2O **5**

Mononuclear complex **5** crystallizes in triclinic crystal system and $P\bar{1}$ space group (Table 1). The asymmetric unit consists of one Cu(II), one $HBCCB^{2-}$, one each of the coordinated and co-crystallized water molecules. Each Cu(II) is four-coordinated with a distorted square planar geometry, completed by nitrogen (N1) from the $HBCCB^{2-}$, two oxygen from different carboxylates of $HBCCB^{2-}$ (O3 and O5) and one coordinated H_2O molecule (O7) (Fig. 6a). The Cu–O bond lengths are in the range [1.922(2)–1.927(2) Å] and Cu–N bond length is 2.047(3) Å, while various angles about the metal center fall in the range [84.70(10)–172.49(12)°] (Table 2). Water molecule present in the lattice is separated from Cu(II) center by ~3.965 Å. (Fig. 6a). Notably, carboxyphenyl group of the ligand is uncoordinated. The *trans*-angles O3–Cu1–O5/N1–Cu1–O7 are 158.82(10)/172.49(12)° while *cis*-close to 90° suggesting distorted square planar geometry about the Cu(II) center. Distortion in geometry may be attributed to very strong interaction between the Cu1 and Cl1 with a Cu1–Cl1 distance of 2.754(14) Å [34]. Such an interaction between copper and chlorine atom attached to aromatic ring is rare and could be considered as coordination bond (Fig. 6a and b). This strong interaction between is reflected by distorted square planar geometry. The overall geometry about Cu(II) center seems very similar to the square pyramidal (*sp*) as suggested by coordination angles (Fig. 6b). The C–H···π interaction in **5** leads to a ladder network incorporating water molecules (Fig. 6c).

3.6. X-ray powder diffraction studies

To acquire information about the structures of **4** and **6**–**8** powder X-ray diffraction studies were made in the limited (2θ, 15–50°) PXRD data set. The powder patterns for these complexes (Fig. 7) were compared with the simulated PXRD data obtained from single crystal X-ray data of **1** and **5**. Patterns in Fig. 7 reveal several diffraction peaks in the range of 15–50° 2θ that have acceptable intensity indicating the bulk purity of samples. There is an acceptable match with some minor differences between the simulated and experimental patterns suggesting that **4** is structurally analogous to **1** and **6**–**8** to **5**.

3.7. Spectral and thermal studies

Detailed description relating to the IR, electronic absorption, and thermal studies are presented in ESI. Fluorescence properties of the Zn(II) and Cd(II) coordination compounds and their potential applications as new luminescent materials have drawn considerable current attention [54–59]. Photoluminescence properties of the free H_3CCB and **1**–**3** have been investigated in solid state at room temperature. Upon excitation at λ, 375 nm the ligand H_3CCB and **2** exhibited strong emissions at 422, and 428, 521 nm,

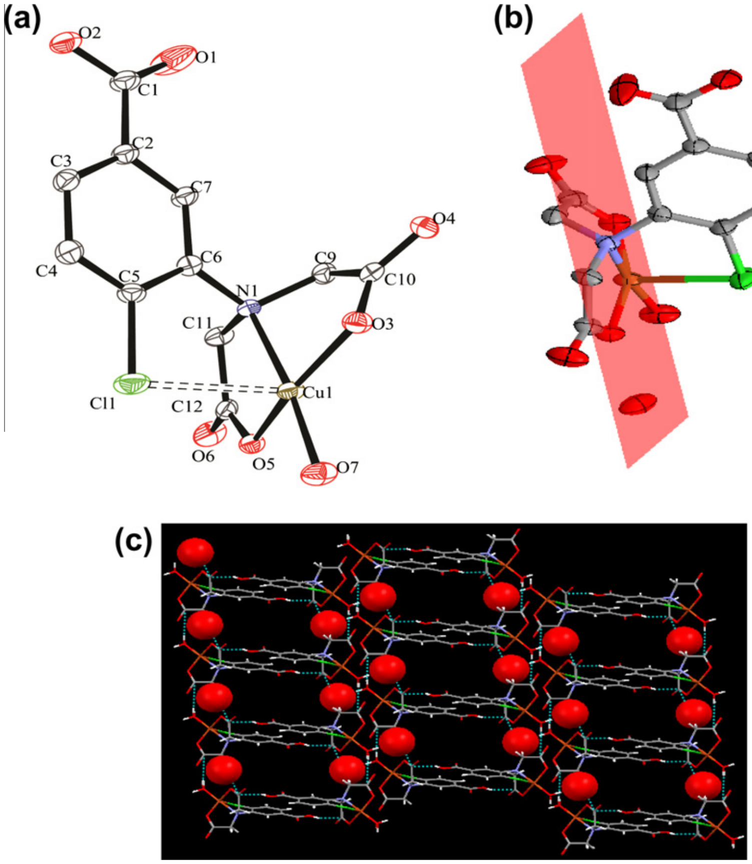

Fig. 6. (a) Crystal structure of **5** (hydrogen atoms omitted for clarity), Symmetry code: $x, 1 + y, z$. (b) View of **5** showing that Cu (II) is in the same plane of coordinated atoms. (c) Ladder view incorporating water molecules in **5** resulted by CH$\cdots\pi$ interactions along crystallographic-'*b*' axis.

Table 2
Selected bond lengths (Å) and angles (°) in **1**–**3** and **5**.

Complex ***1***					
Co–O1	2.057(3)	Co–O4	2.049(3)	Co–O5	2.084(4)
Co–O6	2.121(4)	Co–N1	2.249(4)	C1–O2	1.235(6)
C8–Cl1	1.748(5)	C2–N1	1.484(6)	C1–O1	1.265(5)
N1–C2–C1	113.4(4)	Co1–O1–Co1	101.4(1)	O1–Co1–O1	78.6(1)
O5–Co1–O6	86.6(2)	O4–Co1–O6	179.2(2)	O1–Co1–O1	78.6(1)
O4–Co1–N1	91.5(1)	O2–C1–O1	125.4(4)	C3–N1–Co1	114.5(3)
Complex ***2***					
Zn1–O1	2.090(4)	Zn2–O9	2.094(4)	Zn2–O3	2.031(4)
Zn1–O11	2.065(4)	Zn1–O5	2.054(4)	Zn1–O6	2.179(4)
Zn2–O8	1.984(4)	Zn2–O7	2.352(4)	Zn1–N1	2.208(5)
C1–O2	1.236(6)	C1–O1	1.268(6)		
N2–C11–C10	112.4(4)	Zn1–O1–Zn2	103.5(2)	O4–C9–O3	126.2(5)
O5–Zn1–O11	95.6(2)	O8–Zn2–O7	87.7(2)	O3–Zn2–O7	173.4(2)
O11–Zn1–N1	92.5(2)	O2–C1–O1	124.8(5)	C3–N1–Zn1	115.2(3)
Complex ***3***					
Cd1–O1	2.349(8)	Cd1–O7	2.63(1)	Cd1–O8	2.310(9)
Cd1–O3	2.541(9)	Cd1–O4	2.33(1)	Cd1–N1	2.651
Cd2–O9	2.357(8)	Cd2–O12	2.22(1)	Cd2–O11	2.21(1)
C1–O2	1.29(1)	C10–O6	1.21(2)		
N2–C11–C10	115.4(11)	O1–C1–O2	124.8(12)	O7–Cd1–O8	52.3(4)
O1–Cd1–O5	74.9(3)	O4–Cd1–O1	129.6(3)	O3–Cd1–O7	162.0(3)
O5–Cd1–N2	68.1(3)	N2–Cd1–N1	154.9(3)	Cd2–O9–Cd2	99.9(3)
O9–Cd2–O9	80.1(3)	O13–Cd2–O12	97.0(4)	O13–Cd2–O10	178.3(4)
O4–C9–O3	119.3(12)				
Complex ***5***					
Cu1–O5	1.922(2)	Cu1–O3	1.924(2)	Cu1–O7	1.927(2)
Cu1–N1	2.047(3)	Cu1–Cl1	2.7535(14)	O5–Cu1–O3	158.82(10)
O5–Cu1–O7	93.98(10)	O3–Cu1–O7	97.27(11)	O5–Cu1–N1	86.47(10)
O3–Cu1–N1	84.70(10)	O7–Cu1–N1	172.49(12)	O5–Cu1–Cl1	85.86(8)
O3–Cu1–Cl1	110.82(8)	O7–Cu1–Cl1	95.15(10)	N1–Cu1–Cl1	77.40(8)

Table 3
Selected hydrogen bonds geometry (Å, °) in **1**–**3** and **5**.

D–H···A	D···H	H···A	∠DHA	D···A
*Complex **1***				
N1–H1···O2	0.86	2.49	134	3.154(5)
O5–H5A···O3	0.82	1.85	146	2.570(5)
O5–H5B···O2	0.86	2.25	163	3.056(5)
O6–H6A···O2	0.82	1.97	176	2.785(6)
O6–H6B···O5	0.82	2.60	115	3.033(6)
O6–H6B···O6	0.82	2.33	146	3.048(7)
*Complex **2***				
O5–H5A···O10	0.82	2.23	150	2.967(6)
O6–H6A···O10	0.82	2.01	175	2.830(6)
O7–H7···O2	0.82	1.95	162	2.740(6)
*Complex **3***				
O10–H10···O7	0.82	1.91	165	2.709(4)
O11–H11···O7	0.82	1.96	146	2.815(5)
O12–H12···O2	0.82	2.16	137	2.816(3)
O13–H13···O3	0.82	2.01	136	2.667(6)
*Complex **4***				
O(2)–H(2)···O(4)	0.82	1.83	179	2.650(4)
O(7)–H(7A)···O(8)	0.92(4)	1.75(4)	177(5)	2.669(4)
O(7)–H(7B)···O(6)	0.90(4)	1.78(4)	165(4)	2.661(4)
O(8)–H(8A)···O(5)	0.77(6)	2.15(6)	159(5)	2.883(4)
O(8)–H(8B)···O(4)	0.76(5)	2.01(6)	170(6)	2.765(5)

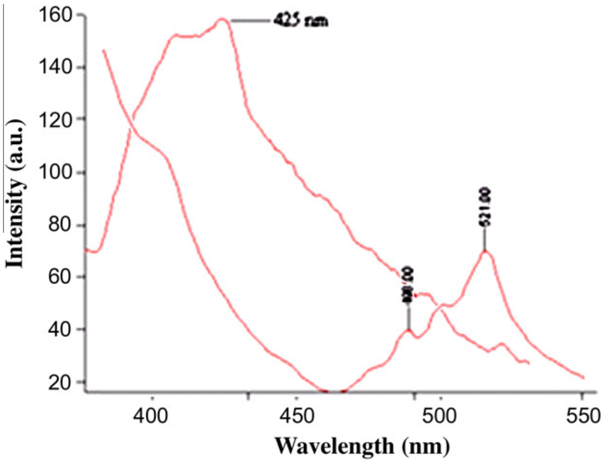

Fig. 8. Solid-state fluorescence spectra of H_3CCB (λ_{ex} 375, λ_{em}, 425 nm) and **2** (λ_{ex} 375, $\lambda_{em,}$ 422, 520 and 542 nm) at rt.

respectively. On the other hand, **1** and **3** weakly emit at 422, 520 and 426, 520, and 542 nm (Fig. 8 and S11). The emission band centered at 422 nm in the uncoordinated ligand may be ascribed to the intra-ligand (ICT) transitions. Therefore, the bands at ~520, 542 nm in the emission spectra of **1**–**3** may be attributed to LMCT (ligand to metal charge transfer) transitions [58,59]. Further, **1**–**3** exhibit red shifted emissions (>500 nm) in comparison to the uncoordinated ligand, which may probably be due to σ-donation from H_3CCB to the metal(II) core. Fluorescence response of H_3BCCB and **5** were examined in water (1×10^{-4} M, Fig. 9). Upon excitation at 325 nm H_3BCCB displays a weak fluorescence at ~445 nm, while excitation at its absorption wavelength (λ_{ex} 242 nm) did not exhibit significant emission. Complex **5** displayed emission bands at 441 nm upon excitation at 325 nm. Fluorescence intensity in **5** is almost three times greater than H_3BCCB, which may be attributed to the reduction of n–π^* transitions due to complex formation with Cu(II) ion.

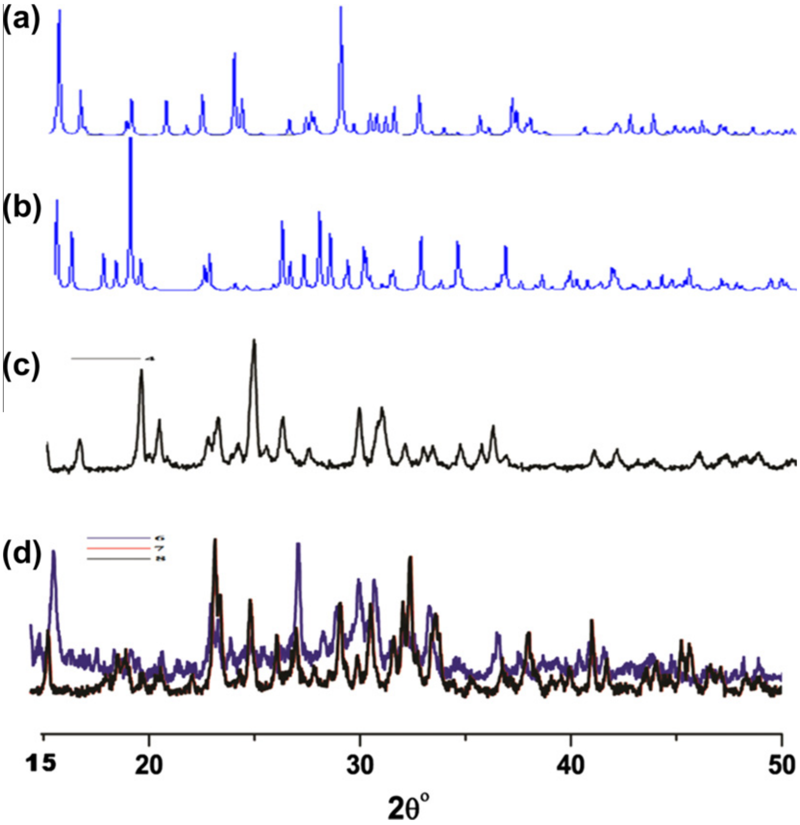

Fig. 7. Experimental powder XRD patterns of **6**–**8** (d) simulated with the PXRD pattern obtained from single crystal X-ray data of **5** (b) and **4** (c) simulated with the pattern single crystal X-ray data of **1** (a).

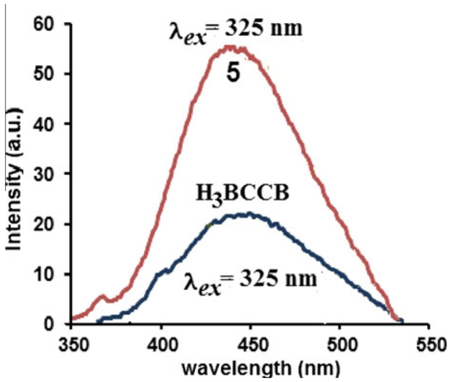

Fig. 9. Fluorescence spectra of H_3BCCB (λ_{ex} 325, $\lambda_{em,}$ 445 nm) and **5** (λ_{ex} 325, $\lambda_{em,}$ 441nm) in water at rt.

4. Conclusions

In summary, through this work we have successfully synthesized four novel coordination polymers using a new aminocarboxylate ligand H_3CCB and four mononuclear complexes based on H_3BCCB. Spectral and structural studies suggested that the synthesis of a variety of coordination polymers can be achieved in the same solvent under analogous reaction conditions. Further, it has been demonstrated that in **1** and **2** the metal centers are bridged by $HCCB^{2-}$ to form a rigid double stranded 1D chain. In these systems the O–H···O hydrogen bonding, C–H···π and π···π interactions construct 2D supramolecular networks possessing square and ellipsoidal cavities of different size. On the other hand, **3** exhibited inclusion of cadmium dimer governed by eight coordinated cadmium coordination polymer. In this system, a 3D supramolecular network resulted from O–H···O hydrogen bonding interactions between dimeric unit and double stranded polymeric chain. The C–H···π and π···π interactions led to 2D parallel double layers incorporating dimeric complex. Thermal studies indicated higher stability of **2** in comparison to **1** and **3**. Further, four mononuclear complexes based on H_3BCCB have been prepared and the representative complex **5** structurally characterized. Significant fluorescence behavior of H_3CCB and **1**–**3** has been observed in solid state, where the intensity of ligand is strong relative to the complexes. Likewise, H_3BCCB and **5** also fluoresces at room temperature.

Acknowledgments

Thanks are due to the Department of Science and Technology, New Delhi, India for financial support through the scheme SR/S1/IC-15/2006. One of the authors (R.P.), thanks the Council of Scientific and Industrial Research, New Delhi, India for a Senior Research Fellowship. We are also grateful to the Department of Chemistry, Faculty of Science, Banaras Hindu University, Varanasi, India for extending laboratory facilities and the National Institute of Advanced Industrial Science and Technology (AIST), Osaka, Japan for single crystal X-ray diffraction facility.

Appendix A. Supplementary material

^1H NMR spectra of the ligands H_3CCB and H_3BCCB, figures for supramolecular assemblies in **1**–**3**, TG-DSC curves for **1**–**3** and fluorescence spectra of **1** and **3**. CCDC 743407, 747607, 747608 and 787720 contain the supplementary crystallographic data for (**1**), (**2**), (**3**) and (**4**). These data can be obtained free of charge from The Cambridge Crystallographic Data Centre via www.ccdc.cam.ac.uk/data_request/cif. Supplementary data associated with this article can be found, in the online version, at doi:10.1016/j.ica.2011.06.018.

References

[1] P. Przychodzén, T. Korzeniak, R. Podgajny, B. Sieklucka, Coord. Chem. Rev. 250 (2006) 2234.
[2] A. Beghidja, P. Rabu, G. Rogez, R. Welter, Chem. Eur. J. 12 (2006) 7627.
[3] R. Wang, J. Zhang, L. Li, Inorg. Chem. 48 (2009) 7194.
[4] R. Fu, S. Xiang, S. Hu, L. Wang, Y. Li, X. Huang, X. Wu, Chem. Commun. 42 (2005) 5292.
[5] W. Yang, X. Lin, A.J. Blake, C. Wilson, P. Hubberstey, N.R. Champness, M. Schröder, Inorg. Chem. 48 (2009) 11067.
[6] Takamizawa, T. Saito, T. Akatsuka, E.-I. Nakata, Inorg. Chem. 44 (2005) 1421.
[7] J.S. Seo, D. Whang, H. Lee, S.I. Jun, J. Oh, Y.J. Jeon, K. Kim, Nature 404 (2000) 982.
[8] O. Hallale, S.A. Bourne, K.R. Koch, New J. Chem. 29 (2005) 1416.
[9] D. Bradshaw, J.B. Claridge, E.J. Cussen, T.J. Prior, M.J. Rosseinsky, Acc. Chem. Res. 38 (2005) 273.
[10] S. Kitagawa, K. Uemura, Chem. Soc. Rev. 34 (2005) 109.
[11] K. Uemura, S. Kitagawa, K. Fukui, K. Saito, J. Am. Chem. Soc. 126 (2004) 3817 (and references therein).
[12] A.N. Khlobystov, A.J. Blake, N.R. Champness, D.A. Lemenovskii, A.G. Majouga, N.V. Zyk, M. Schröder, Coord. Chem. Rev. 222 (2001) 155.
[13] M. Eddaoudi, D.B. Moler, H. Li, B. Chen, T.M. Reineke, M. O'Keeffe, O.M. Yaghi, Acc. Chem. Res. 34 (2001) 319.
[14] G.R. Desiraju, Angew. Chem., Int. Ed. 34 (1995) 2311.
[15] R. Kitaura, S. Kitagawa, Y. Kubota, T.C. Kobayashi, K. Kindo, Y. Mita, A. Matsuo, M. Kobayashi, H.C. Chang, T.C. Ozawa, M. Suzuki, M. Sakata, M. Takata, Science 298 (2002) 2358.
[16] R. Matsuda, R. Kitaura, S. Kitagawa, Y. Kubota, R.V. Belosludov, T.C. Kobayashi, H. Sakamoto, T. Chiba, M. Takata, Y. Kawazoe, Y. Mita, Nature 436 (2005) 238.
[17] B.-C. Tzeng, T.-H. Chiu, B.-S. Chen, G.-H. Lee, Chem.-Eur. J. 14 (2008) 5237.
[18] R. Banerjee, A. Phan, B. Wang, C. Knobler, H. Furukawa, M. O'Keeffe, O.M. Yaghi, Science 319 (2008) 939.
[19] T.K. Prasad, M.V. Rajasekharan, Cryst. Growth Des. 8 (2008) 1346.
[20] A.A. Mohamed, A.P. Mayer, H.E. Abdou, M.D. Irwin, L.M. Perez, J.P. Fackler, Inorg. Chem. 46 (2007) 11165.
[21] H. Eddaoudi, M. Li, M. O'Keeffe, O.M. Yaghi, Nature 402 (1999) 276.
[22] S.S.Y. Chui, S.M.F. Lo, J.P.H. Charmant, A.G. Orpen, I.D. Williams, Science 283 (1999) 1148.
[23] B. Kesanli, W. Lin, Coord. Chem. Rev. 246 (2003) 305.
[24] S. Mandal, S. Natarajan, Inorg. Chem. 47 (2008) 5304.
[25] S. Furukawa, K. Hirai, K. Nakagawa, Y. Takashima, R. Matsuda, T. Tsuruoka, M. Kondo, R. Haruki, D. Tanaka, H. Sakamoto, S. Shimomura, O. Sakata, S. Kitagawa, Angew. Chem., Int. Ed. 48 (2009) 1766.
[26] Y. Dai, E. Ma, E. Tang, J. Zhang, Z. Li, X. Huang, Y. Yao, Cryst. Growth Des. 5 (2005) 1313.
[27] S. Paul, R. Clerac, N.G.R. Hearns, D. Ray, Cryst. Growth Des. 9 (2009) 4032.
[28] P.K. Nanda, V. Bertolasi, G. Aromí, D. Ray, Polyhedron 28 (2009) 987.
[29] T. Chattopadhyay, K.S. Banu, S. Chattopadhyay, A. Banerjee, S. Mondal, E. Suresh, D. Das, Inorg. Chem. Commun. 12 (2009) 26.
[30] H. Aghabozorg, N. Ilaie, M. Heidari, F. Manteghic, H. Pasdarb, Acta Crystallogr., Sect. E 64 (2008) m1351.
[31] K.S. Hagen, R. Lachicotte, A. Kitaygorodskiy, J. Am. Chem. Soc. 115 (1993) 12617.
[32] X.-J. Ke, D.-S. Li, J. Zhao, C.-X. Meng, X.-N. Zhang, Q.-F. He, C. Li, Y.-Y. Wang, Inorg. Chem. Commun. 13 (2010) 484.
[33] K.H. Chung, E. Hong, Y. Do, C.H. Moon, J. Chem. Commun. (1995) 2333.
[34] H.-P. Xiao, L.-G. Zhu, Acta Crystallogr., Sect. E 59 (2003) m964.
[35] D.D. Perrin, W.L.F. Armango, D.R. Perrin, Purification of Laboratory Chemicals, Pergamon, Oxford, UK, 1986.
[36] G.M. Sheldrick, SHELXL-97, Program for X-ray Crystal Structure Refinement, Göttingen University, Göottingen, Germany, 1997.
[37] G.M. Sheldrick, SHELXS-97, Program for X-ray Crystal Structure Solution, Göttingen University, Göttingen, Germany, 1997.
[38] A.L. Spek, PLATON, A Multipurpose Crystallographic Tools, Utrecht University, Utrecht, The Netherlands, 2000.
[39] A.L. Spek, Acta Crystallogr., Sect. A 46 (1990) C31.
[40] M.-H. Zeng, X-L. Feng, W.-X. Zhang, X.-M. Chen, Dalton Trans. (2006) 5294.
[41] V.R. Pedireddi, S. Varughese, Inorg. Chem. 43 (2004) 450.
[42] W.M. Singh, J.B. Baruah, Dalton Trans. (2009) 2352.
[43] J.S.M. Samec, J.-E. Backvall, P.G. Andersson, P. Brandt, Chem. Soc. Rev. 35 (2006) 237.
[44] J.H. Choi, Y.H. Kim, S.H. Nam, S.T. Shin, M.-J. Kim, J. Park, Angew. Chem., Int. Ed. 41 (2002) 2373.
[45] R.-Q. Zhong, R.-Q. Zou, D.S. Pandey, T. Kiyobayashi, Q. Xu, Inorg. Chem. Commun. 11 (2008) 951.
[46] R.-Q. Zou, R.-Q. Zhong, M. Du, D.S. Pandey, Q. Xu, Cryst. Growth Des. 8 (2008) 452.
[47] Y. Qiu, Y. Li, G. Peng, J. Cai, L. Jin, L. Ma, H. Deng, M. Zeller, S.R. Batten, Cryst. Growth Des. 10 (2010) 1332.
[48] D.P. Martin, M.R. Montney, R.M. Supkowski, R.L. LaDuca, Cryst. Growth Des. 8 (2008) 3091.

[49] P. Mukherjee, M.G.B. Drew, C.J. Gómez-Garcįa, A. Ghosh, Inorg. Chem. 48 (2009) 4817.
[50] A. Castińeiras, R. Pedrido, Inorg. Chem. 47 (2008) 5534.
[51] T.C. Stamatatos, G.C. Vlahopoulou, C.P. Raptopoulou, A. Terzis, A. Escuer, S.P. Perlepes, Inorg. Chem. 48 (2009) 4610.
[52] S.-L. Li, Y.-Q. Lan, J.-F. Ma, J. Yang, G.-H. Wi, L.-P. Zhang, Z.-M. Su, Cryst. Growth Des. 8 (2008) 675.
[53] L. Wang, W. You, W.C. Huang, Wang, X.-Z. You, Inorg. Chem. 48 (2009) 4295.
[54] L. Fabbrizzi, M. Licchelli, G. Rabaioli, A. Taglietti, Coord. Chem. Rev. 205 (2000) 85.
[55] S.L. Zheng, J.H. Yang, X.L. Yu, X.M. Chen, W.T. Wong, Inorg. Chem. 43 (2004) 830.
[56] T. Hirano, K. Kikuchi, Y. Urano, T. Nagano, J. Am. Chem. Soc. 124 (2002) 6555.
[57] J. Cui, A. Wang, N.L. Edleman, J. Ni, P. Lee, N.R. Armstrong, T. Marks, J. Adv. Mater. 13 (2001) 1476.
[58] R.C. Evans, P. Douglas, C.J. Winscom, Coord. Chem. Rev. 250 (2006) 2093.
[59] S.V. Ganesan, S. Natarajan, Inorg. Chem. 43 (2004) 198.